



# Numerical Simulations of Nonbreaking Solitary Wave Attenuation by a Parameterized Mangrove Forest Model

Didit Adytia<sup>\*</sup>, Semeidi Husrin<sup>2</sup>

<sup>1</sup>School of Computing, Telkom University, Jl. Telekomunikasi 1 Bandung 40257, Indonesia

<sup>2</sup>Research & Development Centre for Marine and Coastal Resources, Agency for Marine & Fisheries Research & Development, Ministry of Marine Affairs & Fisheries - The Rep. of Indonesia, Jl. Pasir Putih II Ancol Timur, Jakarta 14430, Indonesia

<sup>\*</sup>Corresponding author E-mail: [adytia@telkomuniversity.ac.id](mailto:adytia@telkomuniversity.ac.id)

## Abstract

A numerical approach for investigating a nonlinear transformation of tsunami wave attenuation due to mangrove forest was performed. A dispersive nonlinear wave model so-called Optimized Variational Boussinesq Model (OVBM) is used to simulate the propagation of non-breaking solitary waves, representing tsunami waves. The wave damping by mangrove forest is modelled by adding a dissipation term due to bottom roughness in the momentum equation of the OVBM. The accuracy of the model larger than 85% is obtained by comparing results of simulation with experimental data from the hydrodynamic laboratory.

**Keywords:** *Tsunami, Solitary waves, Mangrove Forest, Water Waves, Boussinesq equations.*

## 1. Introduction

Effectiveness of coastal forest vegetation, such as mangrove forest and coastal pines, as a natural barrier against extreme event such as tsunami has been an interesting topic for both scientists and engineers. Some researchers reported that coastal forest may have played an important contribution in reducing tsunami wave height when it reached shore line, as reported by Dahdouh-Guebas et al. (2005) and Danielsen et al. (2005). On contrary, some field observations show that not all coastal forests can effectively reduce tsunami wave impact on coastal areas, see Latief & Hadi (2006). Morton et al. (2010) reported that many coastal forest trees were found uprooted and broken during the 2010 Chilean Tsunami.

There have been many efforts to study the effectiveness of coastal forest, especially red mangrove or *Rhizophora apiculata*, in attenuating tsunami wave, as reported by Harada & Imamura (2000), Istiyanto et al. (2003), Latief & Hadi (2006). The efforts are mostly by conducting series of physical experiments for an approach to derive hydraulic resistance parameters such drag and inertia coefficients for parameterized coastal forest. Husrin et al. (2012) conducted series of laboratory experiments for investigating tsunami wave attenuation by mangrove forest. The focus of the experiments is to introduce a new tree parameterization procedure for mangrove forest and to derive its related hydraulic resistance parameters.

Approaches from numerical simulations have also been conducted by using numerical models, which are mostly based on a non-dispersive Shallow Water Equations (SWE) as the governing equations. The wave dissipation by coastal forest is introduced in the wave model as local Manning roughness coefficients that are inserted as an additional dissipation term in the momentum equation; see Latief & Hadi (2006), and Harada & Imamura (2000).

In this paper, instead of using the SWE as a numerical model, we choose a dispersive, nonlinear Boussinesq type of model so-called Optimized Variational Boussinesq Model (OVBM), see Adytia & Groesen (2010), as a numerical model for investigating tsunami wave attenuation due to mangrove forest. To test the model performance, we reconstruct a physical experiment of solitary, tsunami-like wave that were performed in the Twin Wave Flume of Leichtweiss-Institute (LWI) at the Braunschweig University of Technology (TU-Braunschweig), Germany. A simple adjustment in the current version of OVBM is included in this paper, i.e. an introduction of bottom dissipation to represent mangrove forest in wave model.

The content of this paper is as follows. We describe the physical experiments of solitary wave attenuation by mangrove forest that have been performed in LWI, TU Braunschweig. The section is followed by a brief description of VBM as wave model. Simulations of solitary waves without and with mangrove forest are described in the following section. Finally, some conclusions and recommendations are described in the last section.

## 2. Laboratory Experiment

Series of laboratory experiments have been performed by Husrin et al. (2012) to investigate the effectiveness of mangroves to reduce tsunami wave energy. A physically based parameterization of complex mangrove trees has been done to derive hydraulic resistance parameters of mangrove forest. The proposed parameterization procedure is based on stiff structure assumption in which only roots and trunk are considered. Photos of real mangrove, model and parameterized mangrove model are shown in Fig. 1. The simplified parameterized mangrove model is expected to have similar hydraulic losses as the real mangrove.



Fig. 1: Real mangrove that consists of roots and trunk (left plot), "Real" mangrove models (middle plot) and parameterized mangrove models (right plot).

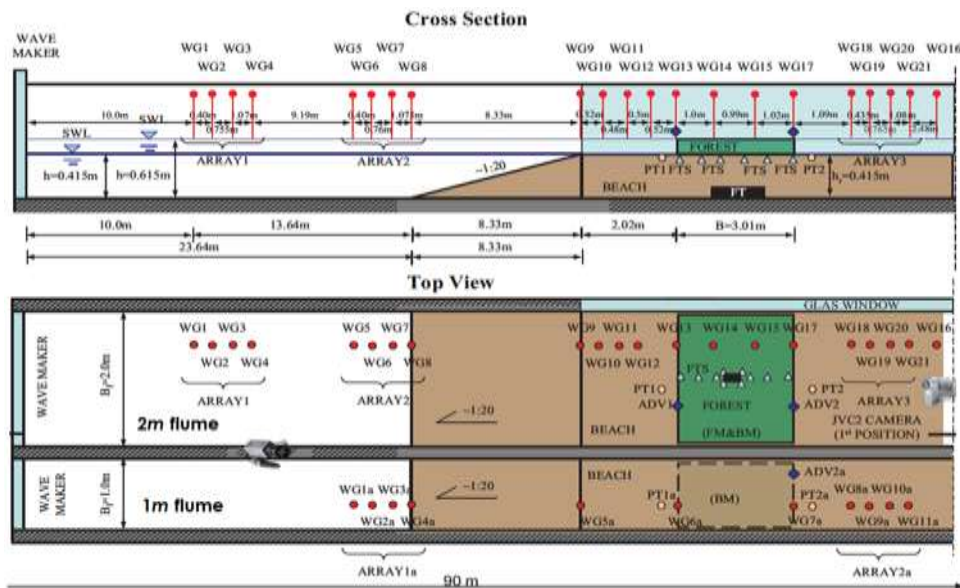


Fig. 2: Experimental set-up in the Twin Wave Flume of Leichtweiss Institute (LWI) with forest width  $B=3\text{m}$  in the 2m-wide flume (Husrin, 2013).

The experiments have been done synchronously in the twin-wave flumes of Leichtweiss - Institute (LWI), TU Braunschweig. The flume consists of 1m and 2m-wide parallel flumes, both approximately 90m and 1.2m high. The 1m-wide flume is without parameterized mangrove forest, while the 2m-wide flume is installed with parameterized mangrove forest model with the scale model 1:25. In the both flumes are installed a sloping bottom (gradient  $\sim 1:20$ ) that is built at 23.64m from the wave maker. The wave maker, located at  $x=0\text{m}$ , generates simultaneous waves in 1m and 2m-wide flumes. There are 21 and 10 wave gauges for measuring wave elevations in the 2m and 1m-wide flume, respectively, see Fig. 2 for the schematic experimental setup. Locations of each wave gauges for 1m and 2m-wide flume are shown in Table 1 & 2, respectively.

Table 1: Wave gauge locations for 1m wide basin (no mangrove forest). The locations are measured from wave maker at  $x=0\text{m}$ .

WG -	1a	4a	5a	6a	7a	8a
x [m]	21.415	23.65	31.98	34	37.01	38.1

Table 2: Wave gauge locations for 2m wide basin (with mangrove forest). The locations are measured from wave maker at  $x=0\text{m}$ .

WG -	2	4	5	8	9	13	17	18
x [m]	10.4	12.225	21.415	23.65	31.98	34	37.01	38.1

Husrin et al. (2012) performs quite many physical experiments with varying wave input, such as solitary wave, regular and irregular waves as well as bores, varying width of mangrove forest, i.e.  $B=0.75, 1.5, 2.25$  and  $3\text{m}$ , and varying water depth which lead to wave breaking locations in the flumes. In this paper, we only investigate a solitary, tsunami-like, wave input that propagates without breaking along the flume, i.e. case number 2009070309 (categorized as Evolution Mode 1 or EM1 category in Husrin et al. (2012)). For the selected case, the wave height and the water depth in the deep are  $0.04\text{m}$  and  $0.615\text{m}$ , respectively. In the next section, we will describe the wave model to be used for simulating solitary wave without and with parameterized mangrove forest.

### 3. Wave Model

In this paper, instead of using a non-dispersive Shallow Water Equations (SWE) as many people used for simulating tsunami, here we use a Boussinesq type of model. The model is so-called Optimized Variational Boussinesq Model (OVBM) that is first introduced by Klopman et al. (2010) and improved by Adytia & Groesen (2012). Unlike the SWE, the VBM takes into account dispersion effects as well as nonlinearity. As described in Adytia & Groesen (2012), the VBM has a tailor-made dispersion properties, which can be set to be sufficiently accurate for simulating desired wave fields, i.e. from long wave such as tsunami, up to short wave such as wind waves (see Adytia (2012), Adytia (2014)). The VBM is implemented numerically by using Finite Element Method (FEM). Recently, the model is extended from weakly nonlinear to fully nonlinear model, see Adytia & Lawrence (2016).

The VBM is derived from the variational principle (see Luke (1967), Zakharov (1968)) that described the water wave as a Hamiltonian system, where the Hamiltonian is the total energy, i.e. the sum of the kinetic and the potential energy. As described in Adytia & Groesen (2012), the VBM is obtained by approximating the vertical structure of the fluid potential  $\Phi(x,y,z,t)$  in the expression of kinetic energy with its value at the surface, denoted by  $\phi(x,y,t)=\Phi(x,y,z=\eta,t)$ , and a linear combination of vertical profile functions  $F_m(z)$  and spatially dependent functions  $\psi_m(x,y)$  as its coefficients:

$$\Phi(x,y,z,t) = \phi(x,y,t) + \sum_m F_m(z) \cdot \psi_m(x,y,t)$$

Here,  $\eta(x,y,t)$  denotes the surface elevation, measured from still water level at  $z=0$ . Vertical functions  $F_m$  have to satisfy conditions in surface as well as in bottom. The functions  $\psi_m$  have to satisfy an optimality condition from kinetic energy that lead to a system of (linear) elliptic equation, see Adytia & Groesen (2012). The weakly nonlinear VBM is described by two dynamic equations, i.e.

$$\partial_t \eta = -\partial_x((h+\eta)\partial_x \phi) - \partial_x(\beta \partial_x \psi) \quad (1)$$

$$\partial_t \phi = -g\eta - (\partial_x \phi)^2 / 2 \quad (2)$$

and one elliptic equation for solving  $\psi_m$ :

$$-\partial_x(\alpha \partial_x \psi) + \gamma \psi = \partial_x(\beta \partial_x \phi) \quad (3)$$

Where  $\alpha, \beta$  and  $\gamma$  are coefficients that depend on vertical profile  $F_m$ . The bottom profile is denoted by  $h(x)$ .

Note that the VBM above does not take into account dissipation by bottom roughness. To use the VBM for simulating wave attenuation by mangrove forest, a dissipation term need to be incorporated in the equations. A commonly used bottom dissipation term in wave model is by using Chezy formulation, that is written in horizontal velocity  $u$ . Since the VBM is written in surface potential  $\phi$ , it is not easy to rewrite the Chezy formula in  $\phi$ , therefore we need to rewrite the VBM in  $u$ -formulation. The VBM in  $u$ -formulation with bottom dissipation is given by

$$\partial_t \eta = -\partial_x((h+\eta)u) - \partial_x(\beta \partial_x \psi) \quad (4)$$

$$\partial_t u = -\partial_x(g\eta - u^2/2) - R_b \quad (5)$$

$$-\partial_x(\alpha \partial_x \psi) + \gamma \psi = \partial_x(\beta u) \quad (6)$$

Where  $R_b = C_f u |u| / (h+\eta)$ , with  $C_f$  is Chezy formula that can be described in Manning's coefficient  $n$  as  $C_f = n^2 g / [(h+\eta)]^{1/3}$ . Note that the dispersion quality of the VBM is completely determined by the choice of vertical profile  $F_m$ . As proposed in Adytia & Groesen (2012), for simulation rather long wave, such as solitary wave in this paper, it is sufficiently accurate to use a parabolic vertical profile for  $F_m$ . Therefore, in this paper we use the parabolic profile as the vertical profile. In the next section, we show results of simulation of OVBM for simulating solitary wave propagation in the setting of physical experiment that has been done by Husrin et al. (2012).

### 4. Numerical Simulations

As described previously, we will only investigate one of many experiments that are performed by Husrin et al. (2012). The selected case number is 2009070309 which is non-breaking case with solitary (tsunami-like) wave input. The generated wave height is  $H_{gen}=0.04m$ , with forest width  $B=3m$ , and water depth of  $h=0.615m$  (in the deep area, before the slope). For numerical simulation, we will use the measured signal at wave gauge WG1 (at  $x=10m$ ) as an influx signal for wave model. Spatial grid spacing is uniform with  $dx=5cm$ .

To test the performance of wave model, we simulate the solitary wave to propagate in a basin without mangrove forest, and then compare results of simulation with measured signal at the 1m-wide flume. The simulation is performed by choosing the Manning coefficient  $n=0$  for the whole domain of computation.

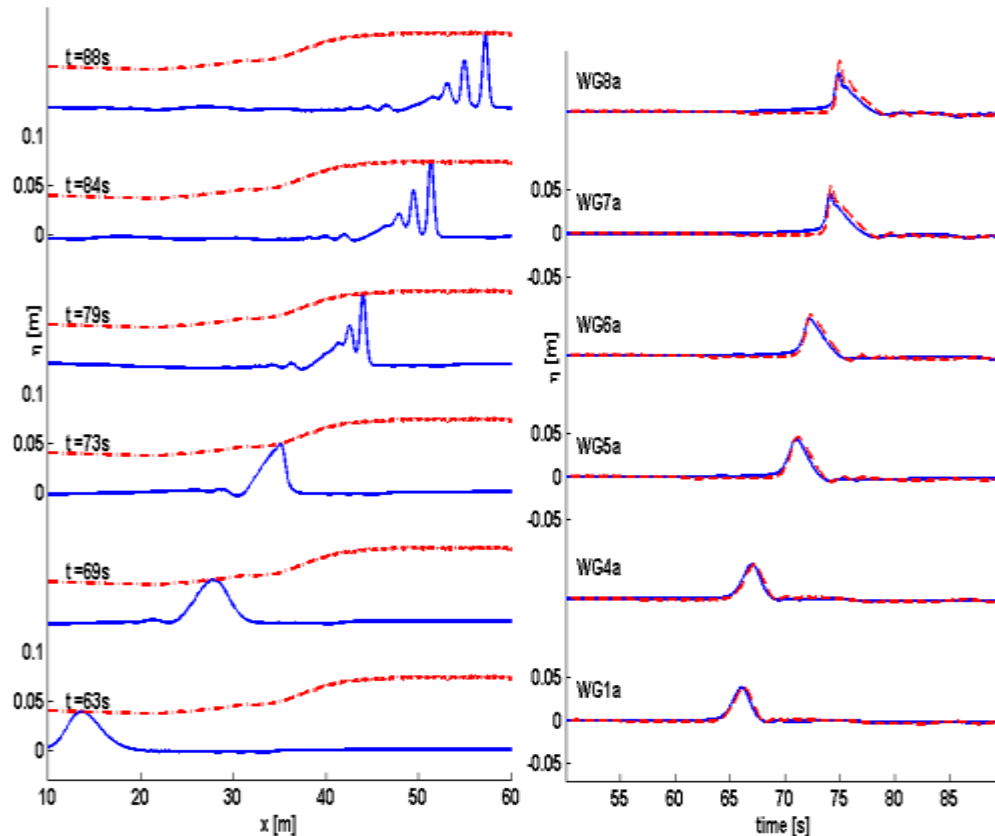


**Fig. 3:** In the left side are plots of simulation's snapshots at  $t=63, 69, 73, 79, 84$  and  $88$ s (from bottom to top). In the right side are plots of signal comparison between simulation (dashed red line) and measurement (solid blue line) at WG = 1a, 4a, 5a, 6a, 7a and 8a for 1m wide basin (no mangrove).

Snapshot of simulations at several times, i.e.  $t=63, 69, 73, 79, 84$  and  $88$ s are shown in left side of Fig. 3. The red dashed lines denote the Maximum Temporal Amplitude (MTA) or maximum wave height during the simulation. Especially for snapshots at  $t=79, 84$  and  $88$ s, it can be seen that the solitary wave is splitting into several solitary waves. This phenomenon is known as soliton splitting, see Pudjapratya et al. (1999). Note that the solitary wave in this case can be viewed as a soliton, since its wave form travels without changing its form, especially in a flat bottom. As the soliton (solitary wave) reaches shallower area, velocities of each wave component of the soliton are changing due to bottom changes; therefore some wave component forms new soliton (solitary) waves. The soliton splitting phenomenon can only be simulated with a dispersive nonlinear wave model. Therefore the SWE cannot simulate the phenomenon.

In the right part of Fig. 3, signal of simulations at several positions are compared with the measured signals. The plots show a good agreement between simulation and experiment in wave height as well as phasing. To quantify signal agreement between the simulation and the measured signal, we define a correlation that is defined as follows

$$\text{corr}(S_1, S_2) = \frac{\langle S_1(t), S_2(t) \rangle}{|S_1(t)||S_2(t)|}$$

Where  $S_1(t)$  and  $S_2(t)$  are the signals to be compared,  $\langle \cdot, \cdot \rangle$  represents the  $L^2$ -inner product, and  $|\cdot|$  the  $L^2$ -norm. The  $\text{corr}(S_1, S_2)$  is a number between  $-1$  and  $1$ , and has value one only when one signal is proportional to the other one. It is used for indicating phase-errors between the two signals. Correlation values between simulation and measured signal are shown in Table 3. It is clear that correlation values are quite high i.e.  $\text{corr} > 0.85$ .

**Table 3:** Correlation values (Corr) between signals of simulation and measurement data for 1m-wide flume or for the case without mangrove forest.

WG -	1a	4a	5a	6a	7a	8a
Corr	0.97	0.97	0.97	0.96	0.94	0.94

To investigate tsunami wave attenuation, we simulate the same solitary wave as in the previous case, but with mangrove forest. The mangrove forest is located from  $x=34$ m to  $x=37$ m with forest width  $B=3$ m. Husrin (2013) derives related Manning roughness coefficient  $n$  for the parameterized mangrove forest from hydraulic resistance parameters, i.e. drag and inertia coefficients. These coefficients are obtained from series of many experiments. He propose the Manning roughness  $n=0.13$  to represent parameterized mangrove forest. For the simulation, we choose the same Manning roughness value to represent mangrove forest.

Fig. 4 shows snapshots at several times (left part) and signal comparison between simulation and measured signal at several wave gauge locations (right part). Location of mangrove forest is indicated by green dash line in the left part of Fig. 4. It is noticeable from the MTA plot that the mangrove forest damped the wave height rather significantly. Since the solitary wave is free again (without damping) after it passes the mangrove forest, the wave height of solitary wave increases again as it propagates in the shallow water. At  $t=84$  and  $88$ s, the solitary wave splits into several solitary waves just as in the previous case, i.e. without mangrove forest.

In the right side of Fig. 4, signals from simulation and measurement are compared at several positions. It shows a good agreement between simulation and measurement in wave height as well as in phasing. Correlation values between simulation and measurement signal at each wave gauges locations are shown in Table 4. It shows acceptable correlation values, i.e.  $\text{corr} \geq 0.85$  for all wave gauge locations.

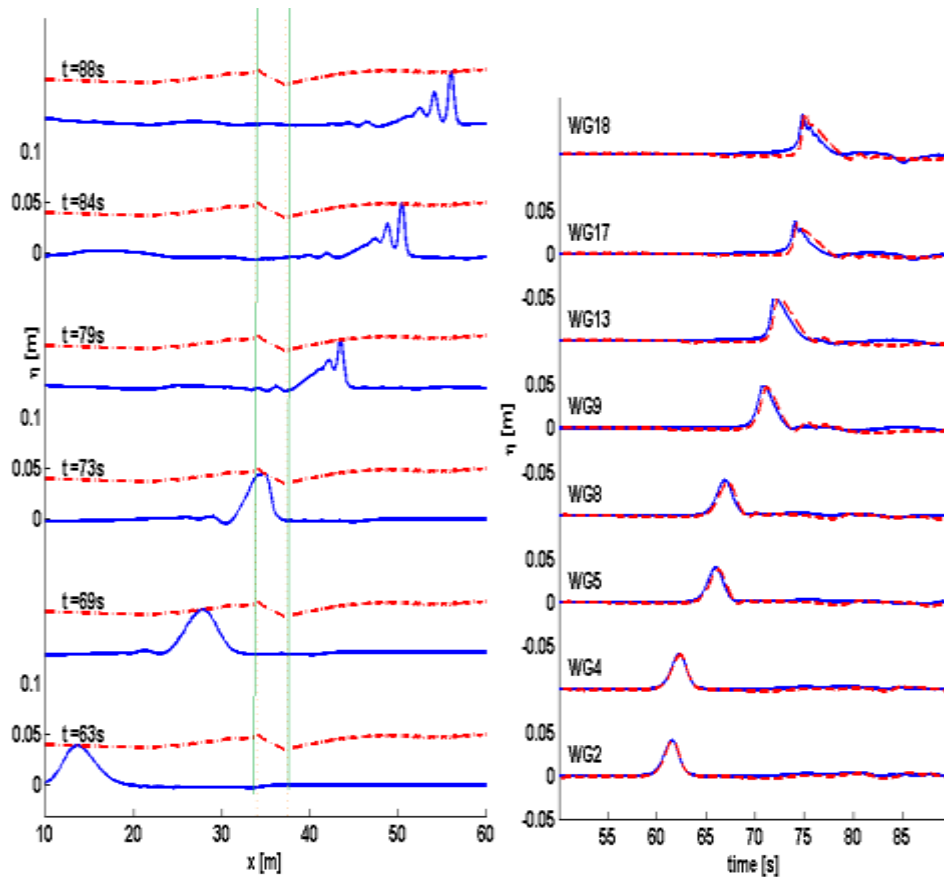


**Fig. 4:** In the left side are plots of simulation's snapshots at  $t=63, 69, 73, 79, 84$  and  $88$  s (from bottom to top). In the right side are plots of signal comparison between simulation (dashed red line) and measurement (solid blue line) at WG= 2, 4, 5, 8, 9, 13, 17 and 18, in 2m width basin (with mangrove forest  $B=3$ m). Green lines indicate the location of mangrove forest.

**Table 4:** Correlation values (Corr) between signals of simulation and measurement data for 2m-width flume or for the case with mangrove forest,  $B=3$ m.

WG -	2	4	5	8	9	13	17	18
Corr	0.95	0.95	0.93	0.94	0.93	0.91	0.85	0.85

## 5. Wave Attenuation

To investigate how wide mangrove forest that is needed for dissipating wave height, we simulate the solitary wave in the previous section (experiment No. 2009070309), with various forest width  $B$ . Here we choose  $B=0$  (no forest), 3, 6, 9, 12 and 24m. From the results of these simulations, we obtained Maximum Temporal Amplitude (MTA) or maximum wave height during simulation time for each cases of  $B$  as shown in Fig. 5. From the plot, for case  $B=0$ m or no mangrove forest, the MTA shows the solitary wave is increasing as the solitary wave is propagating above the slope (from  $x=23.65$ m to  $x=31.98$ m) and after the slope, until to  $x=45$ m. This phenomenon is known as the effect of wave shoaling. After  $x=45$ m, the maximum wave height does not increase as the solitary wave splits into several solitons (solitary waves) as shown in snapshot plots in Fig. 3 at  $t=79, 84$  and  $88$ s.

For cases with mangrove forest  $B=3, 6, 9, 12$  and  $24$ m, the dissipative effects of mangrove forest are compensating the effect of wave shoaling. As shown in Fig. 5, to completely attenuate the wave height of the solitary waves ( $H_{\text{gen}}=0.04$ m or 1m in the prototype), it needs  $B=24$ m of mangrove forest or 600m or forest width in the prototype scale.

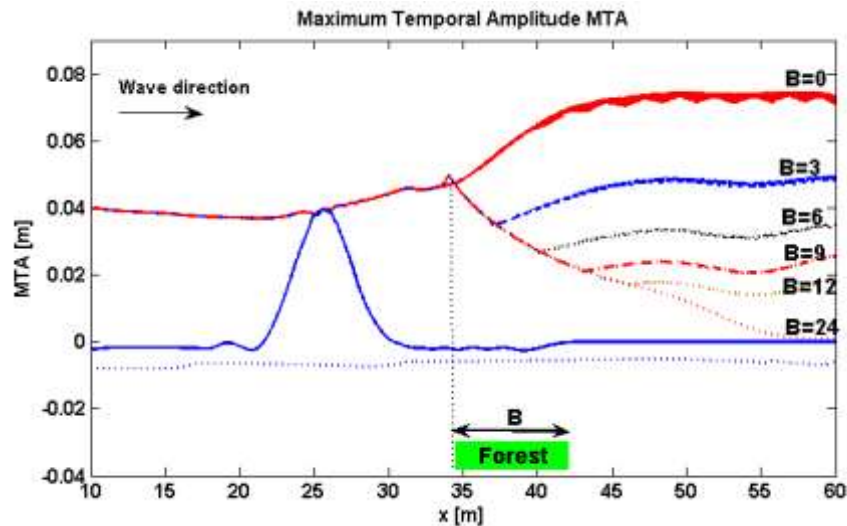


Fig. 5: Maximum temporal amplitude for various forest width  $B = 0$  (no mangrove), 3, 6, 9, 12 and 24m.

To investigate the characteristic of wave height attenuation with respect to the width of mangrove forest  $B$ , we define Wave Height Attenuation  $A$  as follows

$$A = \left[ 1 - \frac{\text{Maximum Wave for } B = 24\text{m}}{\text{Maximum Wave for } B = 0\text{m}} \right] \times 100\%$$

The wave height attenuation  $A=100\%$  means that the wave height is completely dissipated or damped by the mangrove forest. On the other hand,  $A=0\%$  means that the wave height is not dissipated at all. Fig. 6 shows the plot of wave height attenuation  $A$  as a function of forest width  $B$  that is normalized with incoming wave length  $\lambda_0$  for nonbreaking solitary wave (case 2009070309). For this case, the wavelength of the solitary wave is  $\lambda_0 \approx 6\text{m}$ . It can be seen in Fig. 6 that to completely dissipate wave height of the solitary wave ( $A=100\%$ ), it needs forest width with length 4 times the wave length of incoming wave, or  $B \geq 4\lambda_0$ . To dissipate wave height up to 50% of incoming wave height, it needs mangrove forest as wide as incoming wave length ( $B \approx \lambda_0$ ).

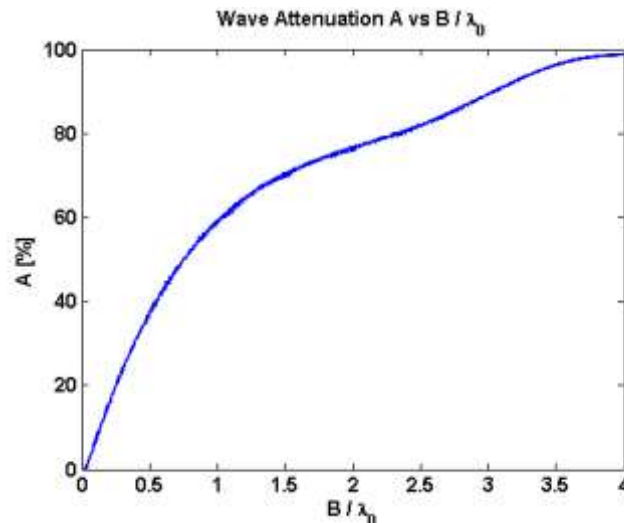


Fig. 6: Wave attenuation  $A$  (in percentage) as function of  $B/\lambda_0$ .

## 6. Conclusion and Discussion

Numerical simulations for investigating tsunami wave attenuation due to mangrove forest have been done by using a dispersive nonlinear wave model, i.e. the OVBM. Wave energy dissipation by the mangrove forest is represented by implementing a bottom friction term in the momentum equation of the VBM. By using a suggested value of Manning roughness for the mangrove forest by Husrin (2012), i.e.  $n=0.13$ , we simulated numerically a physical experiment by LWI, TU Braunschweig, using OVBM. It turns out that the simulation can reconstruct the experiment accurately, with correlation value at all wave gauges are more than 0.85. For a nonbreaking case of the hydrodynamic experiment by Husrin et al. (2012) with a solitary wave as a tsunami wave initiation, we can observe a soliton splitting phenomenon. Unlike the results of SWE simulation (see Husrin (2012)), the soliton splitting phenomenon can be simulated accurately by using the dispersive nonlinear OVBM.

## Acknowledgement

This research is funded by Telkom-University using 'Hibah-Kemitraan' Research Grant 2016-2018. We also would like to acknowledge the Leichtweiss Institute for Hydraulic Engineering (LWI) of TU Braunschweig - Germany for the access to the experimental data of TAPFOR project.

## References

- [1] Adytia, D., and Groesen, E., 2012. Optimized Variational 1D Boussinesq modelling of coastal waves propagating over a slope. *Coast. Eng.*, 64, pp. 139–150.
- [2] Adytia, D., 2014. Simulations of short-crested harbor waves with variational boussinesq modelling. In *Proc.24th Int. Ocean and Polar Engineering Conference. ISOPE 2014, ISOPE*, pp. 912–918.
- [3] Adytia, D., and Lawrence, 2016. Fully nonlinear dispersive HAWASSI-VBM for coastal zone simulations. In *Proc. of the ASME 2016 35th International Conference on Ocean, Offshore and Arctic Engineering OMAE 2016*.
- [4] Broer, L., 1974. On the Hamiltonian theory of surface waves. *Appl. Sci. Res.*, 29(1), pp. 430–446.
- [5] Dahdouh-Guebas, F., L. P. Jayatissa, D. Di Nitto, J. O. Bosire, D. Lo Seen, and N. Koedam, 2005. How effective were mangroves as a defence against the recent tsunami?. *Curr. Biol.*, 15(12), 443–447.
- [6] Danielsen, M.K., Sorensen, M.F. Olwig, V. Selvam, F. Parish, N.D. Burgess, T. Hiralshi, V.M. Karunakaran, M.S. Rasmussen, L.B. Hansen, A. Quarto And N. Suryadiputra, 2005. 'The Asian tsunami: a protective role for coastal vegetation', *Science* 310 p. 643.
- [7] Groesen, E., Adytia, D., and Andonowati., 2008. Near-coast tsunami waveguiding: phenomenon and simulations. *Nat. Hazards Earth Syst. Sci.*, 8, 175–185.
- [8] Harada, K., and Imamura, F., 2006. Effects of coastal forest on tsunami hazard mitigation—a preliminary investigation. *Tsunamis: case studies and recent developments. Advances in Natural and Technological Hazards Research*, pp. 279–292.
- [9] Husrin, S., Strusinska, A, & Oumeraci H., 2012. Experimental study on tsunami attenuation by mangrove forest. *Earth Planets Space*, 64, 973–989.
- [10] Husrin, S., 2013. PhD Thesis: Attenuation of Solitary Waves and Wave Trains by Coastal Forests. University of Braunschweig – Institute of Technology.
- [11] Latief, H., & Hadi, S., (2006): 'Protection from Tsunamis, Coastal Protection in the Aftermath of the Indian Ocean Tsunami': What role for forests and trees?. *Proceedings of the regional technical workshop, FAO, Khao Lak, Thailand*.
- [12] Luke, J., 1967. A variational principle for fluid with a free surface. *J. Fluid. Mech.*, 27, pp. 395–397.
- [13] Morton, RA., Buckley, ML., Gelfenbaum, G., Richmond, BM., Cecioni, A., Artal, O., Hoffmann, C., and Perez, F., 2010. Geological Impacts and Sedimentary Record of the February 27, Chile Tsunami—La Trinchera to Concepcion. *USGS and Chile International Tsunami Survey Team (ITST)*.
- [14] Istiyanto, D.C., Utomo K.S., and Suranto., 2003. Pengaruh Rumpun Bakau Terhadap Perambatan Tsunami di Pantai (The effect of mangrove forest to the attenuation of tsunami in coastal area). *Seminar Mengurangi Dampak Tsunami: Kemungkinan Penerapan Hasil Riset, BPPT – JICA*, 11 March 2003, Yogyakarta (Indonesian).
- [15] Pudjaprasetya, S.R., E. Van Groesen, and E. Soewono. 1999. The splitting of solitary waves running over a shallower water. *Wave Motion*, 29, 375-389.
- [16] Zakharov, V., 1968. "Stability of periodic waves of finite amplitude on the surface of a deep fluid". *J. Epl. Mech.Tech. Phys.*, 9(2), pp. 190–194.